Biochemical Pharmacology 81 (2011) 211–221

Contents lists available at ScienceDirect

Biochemical Pharmacology

journal homepage: www.elsevier.com/locate/biochempharm

Thioredoxin reductase 1 knockdown enhances selenazolidine cytotoxicity in human lung cancer cells via mitochondrial dysfunction

Robyn L. Poerschke, Philip J. Moos *

Department of Pharmacology and Toxicology, University of Utah, L.S. Skaggs Pharmacy, Room 201, 30 S 2000 East, Salt Lake City, UT 84112, USA

ARTICLE INFO

Article history:
Received 16 July 2010
Accepted 27 September 2010

Keywords:
Thioredoxin reductase
Selenazolidine
Selenium
A549
Redox
Apotosis

ABSTRACT

Thioredoxin reductase (TR1) is a selenoprotein that is involved in cellular redox status control and deoxyribonucleotide biosynthesis. Many cancers, including lung, overexpress TR1, making it a potential cancer therapy target. Previous work has shown that TR1 knockdown enhances the sensitivity of cancer cells to anticancer treatments, as well as certain selenocompounds. However, it is unknown if TR1 knockdown produces similar effect on the sensitivity of human lung cancer cells. To further elucidate the role of TR1 in the mechanism of selenocompounds in lung cancer, a lentiviral microRNA delivery system to knockdown TR1 expression in A549 human lung adenocarcinoma cells was utilized. Cell viability was assessed after 48 hr treatment with the selenocysteine prodrug selenazolidines 2-butylselenazolidine-4(R)-carboxylic acid (BSCA) and 2-cyclohexylselenazolidine-4-(R)-carboxylic acid (ChSCA), selenocystine (SECY), methylseleninic acid (MSA), 1,4-phenylenebis(methylene)selenocyanate (*p*-XSC), and selenomethionine (SEM). TR1 knockdown increased the cytotoxicity of BSCA, ChSCA, and SECY but did not sensitize cells to MSA, SEM, or *p*-XSC. GSH and TR1 depletion together decreased cell viability, while no change was observed with GSH depletion alone. Reactive oxygen species generation was induced only in TR1 knockdown cells treated with the selenazolidines or SECY. These three compounds also decreased total intracellular glutathione levels and oxidized thioredoxin, but in a TR1 independent manner. TR1 knockdown increased selenazolidine and SECY-induced mitochondrial membrane depolarization, as well as DNA strand breaks and AIF translocation from the mitochondria. These results indicate the ability of TR1 to modulate the cytotoxic effects of BSCA, ChSCA and SECY in human lung cancer cells through mitochondrial dysfunction.

1. Introduction

Thioredoxin reductase (TR) is a selenoprotein that functions to reduce the oxidoreductase thioredoxin (Trx) in a NADPH-independent manner. Together, this Trx system is an important regulator of cellular redox status. TR is also involved in cell proliferation, DNA replication, cell cycle, transcription factor regulation, and other redox-sensitive cell signaling pathways [1–3] TR contains selenium (Se) in the form of selenocysteine as the penultimate residue at the C-terminus. In humans, TR is found in all tissues and is expressed as two major isoforms: cytosolic (TR1) and mitochondrial.

Many cancers, including non-small cell lung cancer (NSCLC), have high expression levels of both TR1 and Trx. In the lung, TR and Trx expression correlate with cell proliferation, survival, and prognostic factors such as lymph node status and tumor grade [4–6]. TR1 knockdown reversed the malignant phenotype and decreased tumor growth and metastasis of murine lung carcinoma cells further implicating TR1 in cancer development [7]. TR1 was also shown to be involved in the tumor phenotype of malignant cells [1]. Overexpression of the Trx system has been implicated in cell resistance to oxidative and electrophilic insults, including some selenocompounds [8–13]. Thus, TR can protect tumor cells from the oxidative stress generated by many anticancer drugs. These findings indicate a role for the TR system in lung cancer development, progression, and chemoresistance, and identify it as a potential therapeutic target.

Se supplementation trials have had mixed results in regards to cancer incidence and mortality [14–17], but the use of Se in

Abbreviations: AIF, apoptosis inducing factor; ASK1, apoptosis signaling kinase 1; BSO, L-buthionine-(S,R)-sulfoximine; BSCA, 2-butylselenazolidine-4(R)-carboxylic acid; CDDP, *cis*-platinum(II) diammine dichloride; ChSCA, 2-cyclohexylselenazolidine-4(R)-carboxylic acid; Cys, cysteine; DCF, dichlorofluorescein; GSH, glutathione; KEAP1, Kelch-like ECH-associated protein 1; MSA, methylseleninic acid; MTT, 3-(4,5-dimethylthiazol-2-yl)-2,5-diphenyltetrazolium bromide; NAC, *N*-acetyl-L-cysteine; NSCLC, non-small cell lung cancer; NRF2, nuclear factor erythroid 2-related factor 2; *p*-XSC, 1,4-phenylenebis(methylene)selenocyanate; PI, propidium iodide; ROS, reactive oxygen species; Se, selenium; SECY, selenocystine; SEM, selenomethionine; tet, tetracycline; Trx, thioredoxin; TR, thioredoxin reductase.

* Corresponding author. Tel.: +1 801 585 5952; fax: +1 801 585 5111.
E-mail addresses: Robyn.Poerschke@pharm.utah.edu (R.L. Poerschke), philip.moos@utah.edu (P.J. Moos).

0006-2952/$ – see front matter © 2010 Elsevier Inc. All rights reserved.
doi:10.1016/j.bcp.2010.09.024

potential cancer treatment remains of interest. Several selenocompounds have demonstrated anticancer activity in cell culture and *in vivo* studies. Methylseleninic acid (MSA) induces cell cycle arrest and apoptosis in lung cancer cells [18] and is effective at inhibiting xenograft growth [18,19]. The organoselenocompound 1,4-phenylenebis(methylene)selenocyanate (*p*-XSC) has also demonstrated anticancer activity in lung cancer models where selenomethionine (SEM) was not effective [20–22]. Selenocystine (SECY) and two selenazolidine compounds that were designed to non-enzymatically release selenocysteine also decreased murine lung tumors when administered post-initiation [23], but did not affect transcriptional levels of cell cycle or apoptotic genes. Together, these studies indicate that certain selenocompounds exhibit anticancer properties in the lung, though potentially via differential mechanisms that requires elucidation.

Since overexpression of the Trx system contributes to the high antioxidant capacity of NSCLCs, we sought to determine if decreasing TR1 would increase the sensitivity of malignant cells to redox-modulatory selenocompounds. Specifically, the aim of this work was to determine if knockdown of TR1 in A549 human NSCLC cells would affect the cytotoxicity and redox effects of several chemically distinct organoselenocompounds: two selenocysteine prodrug selenazolidines, 2-butylselenazolidine-4(R)-carboxylic acid (BSCA) and 2-cyclohexylselenazolidine-4(R)-carboxylic acid (ChSCA), SECY, MSA, and SEM. A549 cells express some of the highest levels of TR1 as well as other antioxidant genes due to a KEAP1 mutation [24], and therefore, present a unique system to determine role of TR1 in the context of cells with many antioxidant genes overexpressed. For comparison, we also utilized the H1666 human NSCLC cell line, which has lower basal TR1 expression than the A549 cell line and does not have a known KEAP1 mutation [24].

2. Materials and methods

2.1. Reagents

The A549 adenocarcinoma cell line (A549 ATCC) was purchased from American Tissue Type Culture Collection (Manassas, VA). The H1666 adenocarcinoma cell line was a kind gift from Dr. Andrea Bild (University of Utah). BSCA and ChSCA were synthesized as described [25]. L-SEM was from Acros Organics (Morris Plains, NJ), MSA was from PharmaSe, Inc. (Lubbock, TX), and *p*-XSC was from LKT Laboratories, Inc (St. Paul, MN). L-SECY, DMSO, DMF, CDDP, *N*-acetyl-L-cysteine (NAC), tiron, recombinant thioredoxin from *E. coli*, insulin solution from bovine pancreas, iodoacetic acid, iodoacetamide, 40% acrylamide/bis-acrylamide 37.5:1 solution, and ammonium persulfate were purchased from Sigma–Aldrich (St. Louis, MO). Advanced Dulbecco's modified Eagle's medium (DMEM), Glutamax, pcDNA^{TM}6.2-GW/EmGFP-miR, pLenti4/TO/DEST and pLenti6/TR vectors, blasticidin S HCl, Zeocin^{TM}, tetracycline, 3-(4,5-dimethylthiazol-2-yl)-2,5-diphenyltetrazolium bromide (MTT), 2′,7′-dichlorodihydrofluorescein diacetate (H_2DCFDA), propidium iodide (PI), MitoProbe JC-1 assay kit, NuPAGE Bis–Tris gels, APO-BrdU TUNEL assay kit, and bovine serum albumin were from Invitrogen (Carlsbad, CA). CellTiter-Glo Luminescent Cell Viability, MultiTox-Fluor Multiplex Cytotoxicity, GSH-Glo Glutathione, and Caspase-Glo 3/7 assays were purchased from Promega Scientific (Madison, WI). Fetal bovine serum was from HyClone (Logan, UT). Mitochondrial isolation kit for cultured cells, bovine serum albumin standard, Coomassie Plus Protein Reagent, SuperSignal West Dura extended duration substrate, and tris(2-carboxyethyl)phosphine hydrochloride (TCEP HCl) were from Thermo Scientific (Rockford, IL). Primary antibodies directed against TR1, Trx1, AIF, and GAPDH, and polyclonal horseradish peroxidase (HRP)-conjugated secondary antibodies were purchased from Santa Cruz Biotechnology (Santa Cruz, CA); the α-tubulin primary antibody was from Zymed Laboratories (San Francisco, CA). Protease inhibitor cocktail tablets (complete) were from Roche (Indianapolis, IN) and PVDF membrane was from Millipore (Burlington, MA). Western Lighting chemiluminescence reagents were from PerkinElmer Life Sciences (Boston, MA). Nuclear Isolation and Staining Solution (NIM-DAPI) was from Beckman Coulter (Miami, FL). BSO was purchased from Chemical Dynamics Corporation (South Plainfield, New Jersey). JNK inhibitor VIII and p38 MAP kinase inhibitor SB203580 were purchased from Calbiochem (La Jolla, CA) and Upstate Biotechnology (Lake Placid, NY), respectively. The HA-ASK1-wt and HA-ASK1-KM constructs were a kind gift from Dr. Hidenori Ichijo (Tokyo, Japan). The caspase inhibitor, Z-Asp-CH_2-DCB, was from Peptides International (Louisville, KY). Other common reagents were from Sigma-Aldrich (St. Louis, MO), Fisher Scientific (Pittsburgh, PA) or VWR Scientific (West Chester, PA).

2.2. Cell culture

A549 and H1666 cells were cultured in advanced DMEM supplemented with 2% fetal bovine serum and 1% glutamax. When supplemented with serum, advanced DMEM contains ~37 nM Se, primarily in the form of sodium selenite. Cells were maintained at 37 °C in a humidified atmosphere of 5% CO_2. SECY and SEM were dissolved in advanced DMEM. MSA and BSO were dissolved in PBS and CDDP in DMF. All other compounds were dissolved in DMSO. Media was refreshed at the time of treatment and 0.01% DMSO added to MSA, SEM and SECY-treated cells to maintain a constant DMSO concentration amongst treatments. For all experiments other than cell viability, compounds were used at the following concentrations: SEM, 20 μM; MSA, 1 μM; SECY, BSCA, and ChSCA, 5 μM; CDDP, 20 μM.

2.3. Generation of lentiviral miRNA cell lines

microRNA (miRNA) targeted against the TR1 mRNA sequence (NM_003330) beginning at nucleotide 752 was utilized to knockdown TR1 expression (miR-TR1). miRNA targeted at a non-eukaryotic gene (miNeg) was used as a non-knockdown control. Both miRNAs were cloned into pcDNA^{TM}6.2-GW/EmGFP-miR and then cloned into the pLenti4/TO/DEST Gateway vector. A549 cells were transduced with either pLenti4/TO/EmGFP/miR-TR1 or pLenti4/TO/EmGFP/miNeg as well as pLenti6/TR to express tetracycline (tet) repression, creating a tet-inducible miRNA expression system. Stably transduced cells were selected for using Zeocin^{TM} (pLenti4) and blasticidin (pLenti6). Fluorescence-activated cell sorting was used to obtain an enriched EmGFP positive cell population, producing a population with a high percentage of virally transduced cells. Cells were maintained in advanced DMEM.1 μg/mL tet was added to culture medium at least 72 h prior to seeding to induce miRNA expression.

2.4. Measurement of TR activity by NADPH oxidation

Whole cell lysates were collected in lysis buffer. Activity values were measured in duplicate and calculated using the slope of NADPH absorbance at 340 nm at 25 °C over a minimum of 30 min with a Perkin Victor V^3 microplate reader as previously described [26].

2.5. Cell viability by ATP measurement

Cells were seeded into 384-well plates at a density of ~1.25×10^3 cells/well in advanced DMEM and allowed to recover. Drug concentrations ranging from 0 to 60 μM (MSA, *p*-XSC), 0 to

100 μM (CDDP), 0 to 120 μM (SECY), or 0 to 600 μM (SEM, BSCA, ChSCA) were added in advanced DMEM and incubated with cells for 24, 48, or 72 h. For BSO treatments, 20 μM BSO was added to cells at the time of seeding and refreshed every 24 h. For antioxidant treatments, 5 mM NAC or 1 mM tiron was added to cells 2 h prior to seeding. Viability was measured using CellTiter-Glo luminescent reagents as per the manufacturer's instructions. Luminescence was measured using the microplate reader.

2.6. Cell clonogenic assay

Cells were seeded into 6-well plates at a density of 300 cells/well in advanced DMEM. Cells were treated with drug concentrations ranging from 0 to 10 μM (SECY) or 0 to 20 μM (BSCA, ChSCA, MSA) for 7 days. Colonies were stained with MTT for 4 h at 37 °C. MTT concentrations were determined by solubilizing the MTT in 24:1 propanol:HCl and measuring the absorbance at 405 nm using the microplate reader.

2.7. Cell cycle analysis

After 48 h treatments, cells were trypsinized, washed with PBS, resuspended in NIM-DAPI, and incubated for 1 h in the dark. Samples were analyzed using flow cytometry (Cell Lab Quanta SC, Beckman Coulter) with a minimum of 20,000 events recorded for each sample. Cell cycle distributions were estimated using ModFit LT software Version 2.0.

2.8. Immunoblot analysis

For the evaluation of TR1, whole cell lysates were collected as described [27] and protein concentrations determined by the Bradford method. Whole cell lysate was separated by a NuPAGE 10% Bis–Tris gel and transferred to a PVDF membrane. The membrane was blocked in 5% milk in TBS-T, probed with 1:200 anti-TR1 (B-2) monoclonal primary antibody, washed three times with TBST, and probed with 1:5000 donkey anti-mouse horseradish peroxidase (HRP)-conjugated secondary antibodies. For Trx redox status, urea-PAGE and immunoblotting were performed as described [28,29]. For the evaluation of AIF, mitochondrial lysates were isolated from cells using the Mitochondria Isolation Kit for cultured cells with Dounce homogenization protocol. Lysates were sonicated, clarified, and protein concentrations were determined using the Bradford method. Protein was separated by NuPAGE 4–12% Bis–Tris gels, transferred to PVDF membranes and membranes incubated with 1:1000 anti-AIF (H-300) polyclonal primary antibody, washed, and incubated with 1:5000 donkey anti-rabbit HRP-conjugated primary antibody. Protein was detected using chemiluminescence and visualized on a Kodak ImageStation 440.

2.9. Reactive oxygen species

Cells were incubated with 20 μM H_2DCFDA for 20 min at 37 °C following 48 h treatment. Dichlorofluorescein (DCF) and PI fluorescence concentrations were cytometrically determined using a Beckman Coulter Cell Lab Quanta SC flow cytometer as described [27].

2.10. Determination of intracellular glutathione

MultiTox-Fluor reagent was added to wells following 48 h drug treatments and incubated at 37 °C for 30 min. Live-cell fluorescence was measured at 505 nm using the microplate reader. Media was then removed from wells and GSH-Glo reagent containing 1 mM TCEP HCl was added. After incubation at 37 °C for 30 mins, Luciferin Detection reagent was added to each well and incubated for 15 min at 37 °C. Luminescence was measured with the microplate reader. GSH concentrations were calculated from a GSH standard curve and normalized by the MultiTox-Fluor cell viability fluorescence values.

2.11. Cell death assays

Mitochondrial membrane depolarization was assessed using the JC-1 cytometric assay as described [27]. Caspase activity was measured as previously described [28] and luminescence was measured using the microplate reader. DNA fragmentation was measured using the APO-BrdU TUNEL assay kit. Cells were trypsinized, incubated in 1% (w/v) formaldehyde in PBS on ice for 15 mins, washed with PBS, resuspended in cold 70% (v/v) ethanol and placed at −20 °C overnight. Cells were resuspended in 1 mL wash buffer and centrifuged for 5 mins at 250 × *g*. Pellets were resuspended in a DNA-labeling solution containing terminal deoxynucleotidyl transferase and BrdUTP and incubated for 90 mins at 37 °C. Cells were then washed and incubated with 100 μL Alexa Fluor 488 dye-labeled anti-BrdU antibody staining solution for 30 mins at room temperature in the dark, followed by incubation with 0.5 mL PI/RNase A staining buffer. BrdU and PI fluorescence concentrations were measured at 525 and 670 nm, respectively, by flow cytometry.

2.12. Statistical analysis

Data are presented as mean ± standard deviation. One-way ANOVA with Bonferroni post-hoc testing was used to determine statistical significance (GraphPad InStat Version 3.06). $p < 0.05$ was considered significant. Two-way ANOVA with Holm-Sidak post-hoc analysis was used to evaluate the cell cycle analysis (SigmaStat Version 3.5).

3. Results

3.1. TR1 knockdown in A549 cells

TR1 protein expression was decreased by 95% in A549 miR-TR1 cells compared to A549 miNeg cells (Fig. 1A). TR1 knockdown was further confirmed by measuring TR activity via an insulin-dependent NADPH oxidation assay. For A549 miR-TR1 cells, only ~20% TR activity remained (Fig. 1B). The mitochondrial isoform likely contributes to the majority of the remaining TR activity in the miR-TR1 cells, as the NAPDH oxidation assay is not specific for the TR1 isoform. TR activity of A549 miNeg cells did not differ from non-transduced A549 cells (A549 wt). No observable differences in cell viability, morphology, or phenotype existed between the miNeg and miR-TR1 cell lines (Fig. 1C).

3.2. Effects of TR1 knockdown on drug cytotoxicity

Minimal differences in cell viability between A549 miNeg and miR-TR1 cells were observed with 24 hr drug treatments (data not shown). When treatments were carried out for 48 h, decreases in A549 miR-TR1 cell viability were observed with the selenocysteine prodrug selenazolidines BSCA and ChSCA at concentrations of 5–100 μM (Fig. 2) and SECY at concentrations of 1–10 μM. These compounds demonstrated >4-fold increases in sensitivity in the miR-TR1 cells compared to the miNeg cells. We also assessed the toxicity of the methylselenol precursor methylseleninc acid (MSA) and the selenoamino acid SEM, but did not find differential toxicity with TR1 knockdown using treatment times up to 72 h (72 h data not shown). This lack of TR1-dependent sensitivity with SEM in A549 cells is consistent with effects observed with these compounds in colon cancer cells [12]. We also determined if

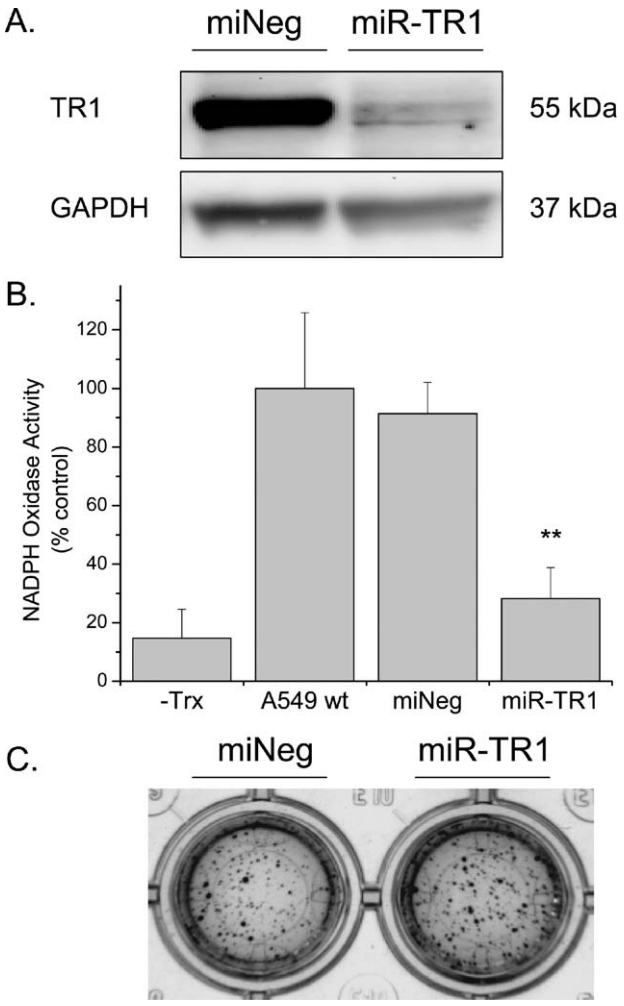

Fig. 1. Knockdown of TR1 in A549 miR-TR1 cells by miRNA. A549 cells were transduced with lenitviral miRNA constructs to produce miNeg and miR-TR1 cell lines (see Section 2). Cells were treated with 1 μg/mL tetracycline for 72 h to induce miRNA expression. (A) Determination of TR1 protein expression by Western blotting. TR1 is the top band of the doublet. GAPDH was probed as a loading control using 1:500 anti-GAPDH polyclonal primary antibody. A similar decrease in TR1 protein expression was observed in A549 miR-TR1 cells up to 72 h after removal of 1 μg/mL tetracycline. The blot shown is representative of two individual experiments. (B) Measurement of TR activity via NADPH oxidation. Data are presented as % A549 wt activity. $n = 2$ for all groups. (*) Indicates $p < 0.05$ versus miNeg. NADPH oxidative activity in A549 cell lysates without added Trx (−Trx) in the reaction mixture, basal activity, activity in miNeg cells, and in the miR-TR1 cells. (C) Anchorage independent growth assay. Cells were allowed to grow in 2% growth factor reduced Matrigel (BD Biosciences; Bedford, MA) and advanced DMEM supplemented with 1 μg/mL tet for 7 days, with media and tet refreshed every three days. Colonies were stained with MTT overnight and visualized on the Kodak ImageStation. No difference in colony growth was observed between the two cell lines. The data shown are representative of six replicates.

TR1 knockdown enhanced the toxicity of *cis*-platinum(II) diammine dichloride (CDDP, cisplatin), as it is a first-line treatment for NSCLC and interacts with TR1. A549 miR-TR1 cells were less than 2-fold more sensitivity to CDDP after 48 hr treatment compared to A549 miNeg cells. These viability data suggest that TR1 can protect against Se toxicity in a compound and cell line dependent manner.

To determine if the observed decreases in ATP content were a consequence of decreased cell proliferation, we conducted a clonogenic survival assay. Colony formation was observed in the miNeg and miR-TR1 cell lines after 7 days of treatment with MSA, SECY, BSCA, or ChSCA. All of these selenocompounds decreased clonogenic survival in a dose dependent fashion; however, replicate experiments did not demonstrate a statistically significant difference between miNeg and miR-TR1 cells. Representative examples of clonogenic survival are displayed in Fig. 3. Taking these data into account with the ATP content viability data supports a mechanism whereby TR1 knockdown enhances SECY and selenazolidine cytotoxicity, but may not increase the sensitivity of A549 cells to these compounds in longer term experiments.

To further evaluate the role of these compounds in cell proliferation, the effects of TR1 knockdown and the selenocompounds that demonstrated a TR1-dependence in the ATP assay were evaluated for alterations in cell cycle population distributions. The effects of TR1 attenuation and selenocompound treatment were statistically significant but represent small shifts in the overall population (Table 1). Still, attenuation of TR1 alone decreased cells in G_1 phase and increased the population in S phase. SECY and the selenazolidines increased cells in G_1 phase, but to a lesser extent in miR-TR1 cells than miNeg cells.

To determine if the selenazolidine-mediated cytotoxicity observed in the A549 cells translated to other non-small cell lung cancer lines, we treated H1666 cells (which do not have a KEAP1 mutation) with the cytotoxic agents SECY and ChSCA. H1666 cells expressed considerably less TR1 than A549 cells (Fig. 4A), and displayed similar sensitivity to the cytotoxicity of these agents (Fig. 4B). SECY, which displayed a more modest sensitization in the A549 cells with attenuated TR1, displayed comparable cytotoxicity in these cells, but ChSCA-dependent cytotoxicity was more similar to the miR-TR1 A549 cells.

3.3. Effects of TR1 knockdown and glutathione depletion on cell viability

As oxidative stress is a major inducer of cell death, we investigated whether TR1 and glutathione (GSH) depletion together decrease cell viability independent of any external insult. To determine the effect of simultaneously depleting these two antioxidant systems, miR-TR1 cells were treated with L-buthionine-(S,R)-sulfoximine (BSO). BSO decreases GSH synthesis via inhibition of gamma-glutamylcysteine synthetase, thereby decreasing the cellular GSH concentration. Treatment of A549 miR-TR1 cells with BSO resulted in decreased cell viability in a time-dependent manner, as a difference in cell viability was observed after 72 h of BSO treatment (Fig. 5). At this time point, BSO decreased miR-TR1 cell viability by 75% but did not affect the viability of miNeg cells.

3.4. Selenocompounds alter redox balance in TR1 knockdown cells

As the greatest differences in cell viability between miNeg and miR-TR1 cells at 48 h were observed at low micromolar concentrations of BSCA, ChSCA, and SECY, we chose 5 μM treatments of these compounds to further investigate their mechanism of cell death specific to miR-TR1 cells. Reactive oxygen species (ROS) were increased 2-fold and 4-fold by the selenazolidines and SECY, respectively, in the miR-TR1 cells (Fig. 6A). No increase in ROS was detected with these compounds in miNeg cells, indicating that TR1 may function in A549 cells to protect against ROS generation observed with these compounds. No change in ROS levels were observed at 48 h with 20 μM SEM or 1 μM MSA. To further evaluate the role of ROS, cells were pretreated with NAC, a thiol antioxidant, or tiron, a non-thiol antioxidant, prior to selenocompound treatment. No attenuation of SECY or selenazolidine cytotoxicity was observed with either NAC or tiron (data not shown).

Since GSH depletion decreased A549 cell viability in combination with TR1 knockdown, we measured total intracellular GSH

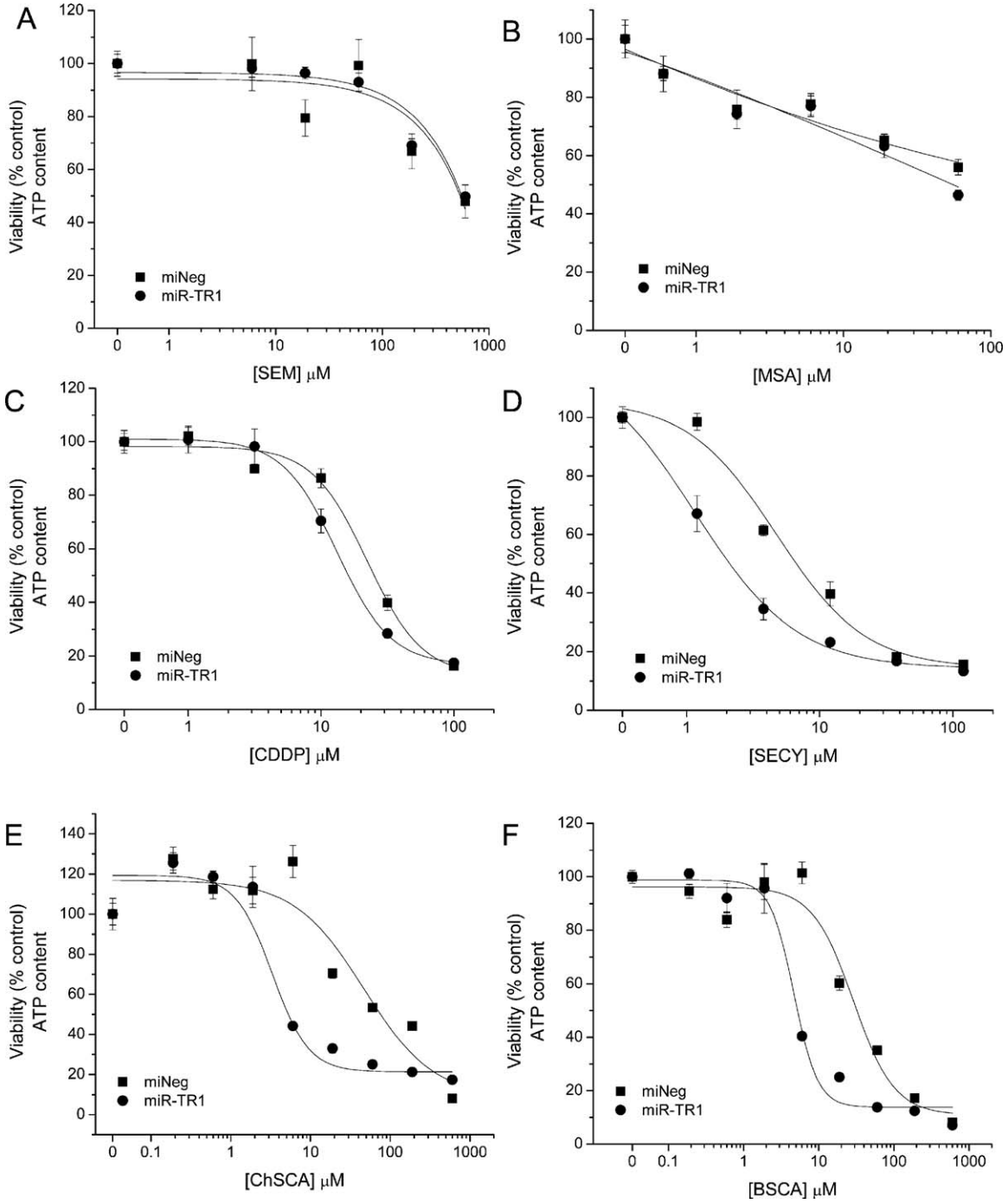

Fig. 2. Effects of TR1 knockdown on drug cytotoxicity in A549 cells. Viability of A549 miNeg (■) and miR-TR1 (●) cells was assessed by measuring cellular ATP content after 48 h drug treatment at the indicated concentrations. Viability values are expressed as % relative to vehicle controls, which were set to 100%. $n = 4$ for all data points. No sensitization was observed in cells treated with (A) SEM or (B) MSA. Sensitization was observed in cells treated with (C) CDDP (miNeg IC_{50}: 22 ± 4 μM; miR-TR1 IC_{50}: 13 ± 0.5), (D) SECY (miNeg IC_{50}: 5 ± 1.4 μM; miR-TR1 IC_{50}: 1.2 ± 0.3), (E) ChSCA (miNeg IC_{50}: 48 ± 8 μM; miR-TR1 IC_{50}: 3 ± 1.1), and (F) BSCA (miNeg IC_{50}: 28 ± 8 μM; miR-TR1 IC_{50}: 5 ± 0.7).

following 48 h drug treatments to determine if decreased GSH was involved in the increased sensitivity of the miR-TR1 cells. No alteration in GSH concentration was observed with TR1 knockdown alone (Fig. 6B). The greatest depletion of total GSH was observed with BSCA, ChSCA, and SECY, as these compounds decreased total intracellular GSH by 90% independent of TR1 status. CDDP also depleted GSH in a TR1 independent manner, but to a lesser extent than that elicited by SECY or the selenazolidines (~40%). Taken together, these data indicate that selenazolidines and SECY can alter the cellular redox balance by generating ROS and depleting total intracellular GSH.

3.5. Selenocompound-induced Trx oxidation

The alterations in ROS and GSH indicative of altered redox balance led us to look at Trx redox status since it can be modulated by oxidative stress and is known to be involved in apoptotic signaling. Trx contains five cysteine (Cys) residues and therefore

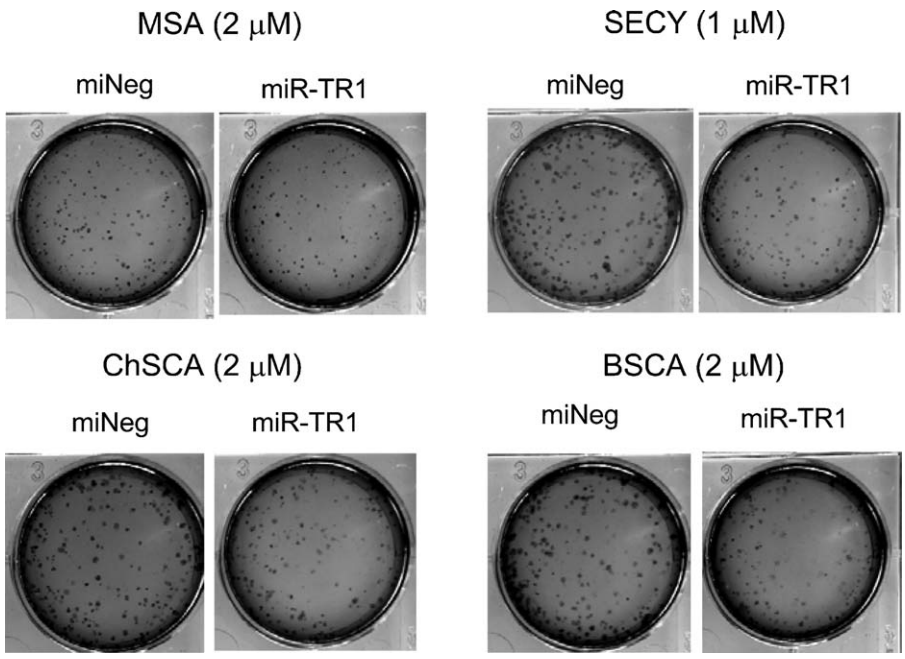

Fig. 3. TR1 knockdown did not increase sensitization in clonogenic survival in A549 cells. Representative images of 7-day selenocompound treatment of A549 cells stained by the addition of MTT to the media and then visualized. Measurements of formazan-converted MTT indicate that statistically significant differences were not obtained between the miNeg and miR-TR1 cells.

can exist in six possible oxidation states. In DMSO-treated miNeg and miR-TR1 cells, TR1 was primarily in the reduced state (Fig. 7; Table 2). This finding that TR1 knockdown alone does not alter the Trx oxidation status of A549 cells is in agreement with reports for other transformed cell lines [28,30]. BSCA, ChSCA, and SECY increased the expression of oxidized forms of Trx, primarily the two residue oxidation state, in a TR1-independent manner. No appreciable expression of Trx in the three highest oxidation states was detected with any of the treatments.

To assess the involvement of Trx oxidation in the cell death mechanism of these selenocompounds, we investigated the apoptotic stimulating kinase 1 (ASK1) pathway. ASK1 is an apoptotic signaling protein that is regulated by the oxidation status of Trx [31,32]. ASK1 associates with Trx^{red}, which prevents its phosphorylation and subsequent activation. When Trx is oxidized, ASK1 dissociates and can be phosphorylated, activating apoptotic pathways involving JNK and p38 MAP kinase. As BSCA, ChSCA, and SECY increased Trx^{ox} levels, we sought to determine if these compounds were inducing cell death through the ASK1 pathway. Prior to selenocompound treatment, cells were transfected with HA-tagged ASK1 wt or kinase mutant (KM) constructs

Table 1
Cell cycle distribution.

		G_1	S	G_2/M
miNeg				
	DMSO	68.0 ± 0.2	24.1 ± 0.6	7.9 ± 0.7
	SECY	75.5 ± 1.4[a]	18.8 ± 0.6[a]	5.8 ± 1.0
	BSCA	73.1 ± 2.0[a]	20.2 ± 1.3[a]	6.7 ± 1.6
	ChSCA	78.3 ± 0.7[a]	18.3 ± 0.9[a]	3.4 ± 1.3[a]
miR-TR1				
	DMSO	64.2 ± 1.5[b]	27 ± 1.0[b]	8.8 ± 1.0
	SECY	69.9 ± 0.5[a,b]	23 ± 1.1[a,b]	7.1 ± 0.7
	BSCA	67.7 ± 0.9[a,b]	25.6 ± 1.2[b]	6.7 ± 0.2
	ChSCA	72.3 ± 2.2[a,b]	22.8 ± 2.0[a,b]	4.8 ± 2.0[a]

Cell cycle distributions are statistically different (two-way ANOVA) both due to selenocompound treatment and the TR1 attenuation ($n = 3$ for all groups). ([a]) Indicates $p < 0.01$ versus matched DMSO vehicle control; ([b]) indicates $p < 0.01$ versus matched miNeg treatment as measured by the Holm-Sidak post-hoc test.

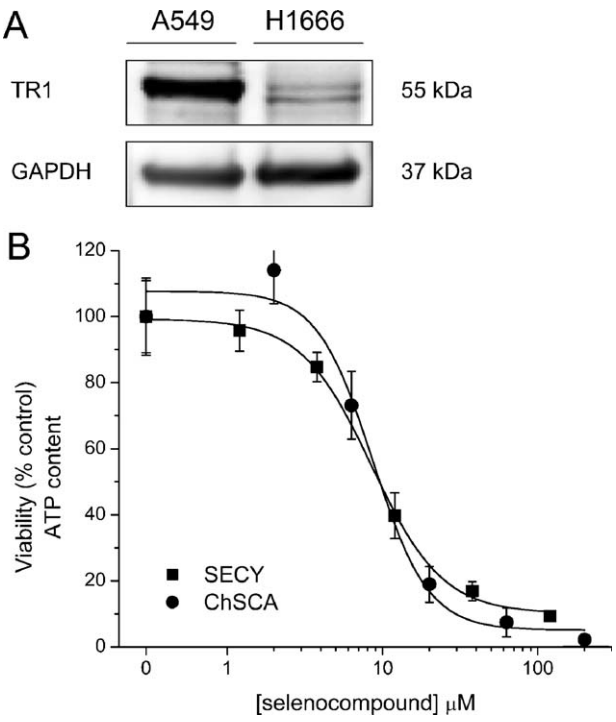

Fig. 4. TR1 expression and selenocompound cytotoxicity in H1666 human NSCLC cells. (A) Determination of TR1 protein expression by Western blotting. 10 μg protein was loaded for each sample. H1666 cells have ~85% less TR1 protein expression than A549 cells as determined by densitometry. (B) H1666 cell viability following 48 h selenocompound treatments. Concentrations ranged from 0 to 200 μM (ChSCA) or 0 to 120 μM (SECY). Viability was assessed by ATP content. Values are expressed as % relative to vehicle controls, which were set to 100%, and $n = 6$ for all data points. Both SECY and ChSCA have similar cytotoxicity (SECY IC_{50}: 8.5 ± 0.6; ChSCA IC_{50}: 8.6 ± 1.7 μM).

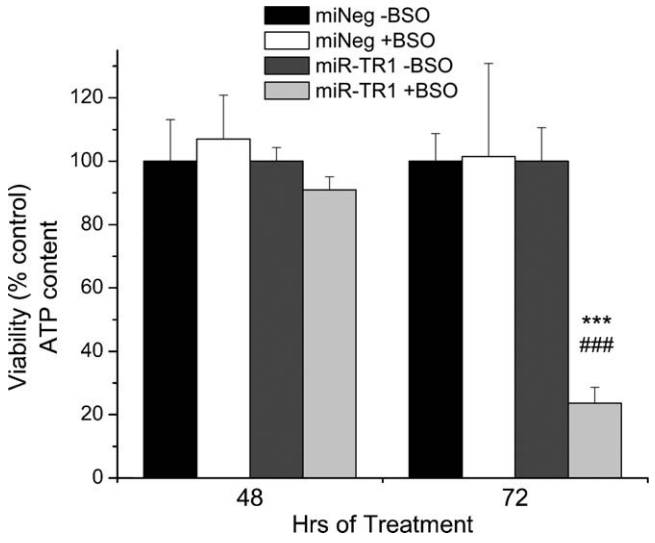

Fig. 5. Effects of TR1 and GSH attenuation on A549 cell viability. miNeg and miR-TR1 cells were treated with 20 μM BSO or PBS vehicle for 48 or 72 h. Cell viability was determined by measuring cellular ATP content. BSO-treated viability values are expressed as % matched vehicle controls. $n = 8$ for all groups. (***) Indicates $p < 0.001$ versus −BSO (control); (###) indicates $p < 0.001$ versus 48 h miR-TR1 +BSO.

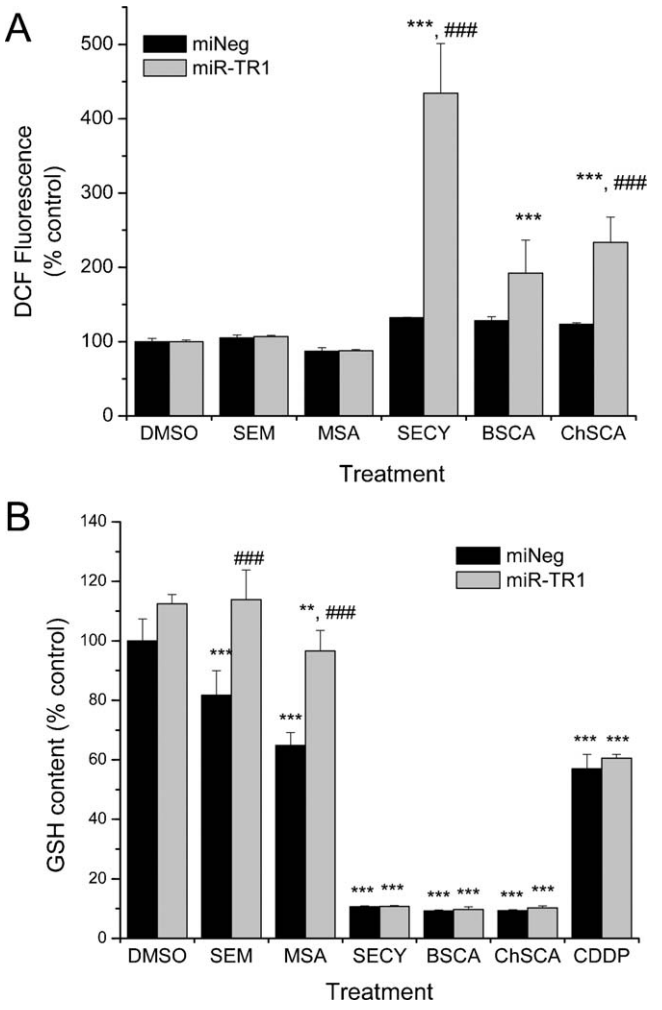

Fig. 6. Assessment of cellular redox status parameters. Treatments were for 48 h at the following concentrations: SEM, 20 μM; MSA, 1 μM; SECY, BSCA, and ChSCA, 5 μM; CDDP, 20 μM. (A) DCF fluorescence concentration. (B) Measurement of total intracellular GSH. GSH concentration values were normalized to cell viability fluorescence values and are expressed as % miNeg DMSO control. $n = 3$ for all DCF assay treatment groups; $n = 4$ for GSH assay treatment groups. (**) Indicates $p < 0.01$ versus matched DMSO vehicle control; (***) indicates $p < 0.001$ versus matched DMSO vehicle control; (###) indicates $p < 0.001$ versus matched miNeg treatment.

[31] or treated with 55 nM JNK inhibitor VIII or 600 nM p38 MAP kinase inhibitor SB203580. Despite the increased Trx oxidation observed in both cell lines with the selenazolidines and SECY, there was no effect of the ASK1 KM, JNK inhibition, or p38 inhibition on selenocompound-induced cell death (data not shown). These findings suggest that although the selenazolidines and SECY alter Trx redox status, they do not induce cell death through the ASK1 pathway.

3.6. Mitochondrial dysfunction in the mechanism of selenocompound-induced cell death

To verify that the selenocompounds were inducing cell death and not simply depleting cellular ATP, mitochondrial membrane potential was assessed using the JC-1 assay. TR1 knockdown alone did not affect the mitochondrial membrane potential as there was no difference in the polarized and depolarized populations of miNeg and miR-TR1 DMSO-treated cells (Fig. 8). TR1 knockdown sensitized the A549 cells to mitochondrial depolarization induced by the selenazolidines, as an increase in the depolarized mitochondrial population was only observed with these compounds in the miR-TR1 cells. Knockdown also further sensitized cells to depolarization by SECY. Although 1 μM MSA did not induce cell death as assessed by ATP content, MSA-treated miR-TR1 cells had a greater depolarized mitochondria population than MSA-treated miNeg cells, but this population was not statistically different from DMSO-treated miR-TR1 cells. Consistent with the

Table 2
Summary of Trx oxidation states.

Cell type	Redox state	Treatment					
		DMSO	SEM	MSA	SECY	BSCA	ChSCA
miNeg							
	4 (ox)	4.4 ± 1.6	6.3 ± 4.5	4.5 ± 0.5	25 ± 2.7	26 ± 1	34 ± 0.1
	5	5.6 ± 1.8	8.1 ± 3.3	5.5 ± 2.2	11 ± 5	9.6 ± 1.8	9.5 ± 2.9
	6 (red)	90 ± 3.4	85 ± 7.8	90 ± 2.6	64 ± 8.4	64 ± 2.9	56 ± 3.4
miR-TR1							
	4 (ox)	7.4 ± 0.2	6.3 ± 1.7	4.9 ± 0.5	22 ± 4.9	28 ± 4	33 ± 8.7
	5	5.9 ± 2.5	4.2 ± 1.1	4.4 ± 1	9.9 ± 1.2	7.3 ± 2.9	9.2 ± 0.8
	6 (red)	87 ± 2.3	89 ± 2.8	91 ± 0.5	68 ± 3.4	64 ± 0.8	57 ± 7.8

Relative band intensities from the Trx oxidation state immunoblot analysis (example in Fig. 5) were quantified using densitometry. Three of the six possible oxidation states (the reduced state = 6 (red), one cysteine oxidized = 5, or two cysteines oxidized = 4 (ox)) were detected at relative band intensities greater than 1%. The data are presented as the mean percent relative net band intensities ± standard deviations. $n = 3$ for all samples.

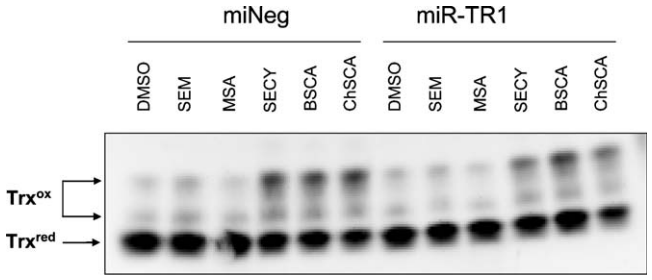

Fig. 7. Selenocompounds induce expression of Trx in an oxidized state. Iodoacetic acid/iodoacetamine-labeled samples were collected following 48 h treatments at the following concentrations: SEM, 20 μM; MSA, 1 μM; SECY, BSCA, and ChSCA, 5 μM. Equal amounts of protein were analyzed by urea-PAGE and transferred to PVDF membranes that were probed with 1:200 anti-Trx primary antibody. Bands correspond to reduced Trx (bottom band) or Trx in various oxidation states (upper two bands). SECY, BSCA, and ChSCA increased the expression of Trx in an oxidized state in both A549 miNeg (left six lanes) and miR-TR1 (right six lanes) cells. The blot shown is representative of at least two independent experiments.

lack of effects on cytotoxicity and redox parameters in either cell line, SEM did not alter the mitochondrial membrane potential. These finding suggest that the selenocompounds are indeed inducing cell death, as mitochondrial membrane depolarization is a hallmark of the cell death process.

3.7. Caspase-independent mechanism of cell death involving DNA fragmentation

We investigated the ability of selenocompounds to induce DNA fragmentation using the TUNEL assay to further elucidate the mechanism of cell death. ChSCA and SECY induced DNA strand breaks, but only with TR1 knockdown (Fig. 9A). Surprisingly, BSCA did not produce significant DNA fragmentation with 48 h treatment despite its ability to decrease cellular ATP content and depolarize the mitochondrial membrane. We sought to further characterize SECY and the selenazolidines by determining if they induce cell death in the miR-TR1 cells through a caspase-dependent pathway. Although these compounds elicit mitochondrial membrane depolarization and DNA strand breaks, no increase in caspase 3/7 activity was observed (Fig. 9B) and selenocompound cytotoxicity was not attenuated when a broad spectrum caspase inhibitor (Z-Asp-CH_2-DBM) was used (data not shown).

Since there was no indication of caspase activation, we looked for evidence of a caspase-independent mechanism of cell death involving apoptosis inducing factor (AIF). AIF is a mitochondrial protein that translocates to the nucleus upon mitochondrial outer membrane permeabilization, where it induces DNA fragmentation and ultimately apoptosis independent of caspases [33]. Decreased AIF expression in the mitochondrial fraction was observed in miR-TR1 cells with 48 h selenazolidine and SECY treatments as determined by Western blotting (Fig. 9C). This decreased AIF expression is indicative of AIF translocating from the mitochondria to the nucleus. Taken together, these data suggest that caspase-independent AIF activation is involved in the cell death mechanism of the selenazolidines and SECY at low micromolar concentrations in A549 miR-TR1 cells.

4. Discussion

Lung cancer has the highest mortality rate of all cancer types, with a five year survival rate of only 16% [34]. One reason for this poor survival rate is the low success rate of current treatments. We utilized the A549 human NSCLC cell line as a model of lung carcinoma to further determine the effects of TR1 expression on drug sensitivity. This cell line was chosen because A549 cells have one of the highest overexpression levels of TR1 compared to human bronchial epithelial cells [4]. Additionally, the negative regulator of nuclear factor erythroid 2-related factor 2 (NRF2), Kelch-like ECH-associated protein 1 (KEAP1), is mutated in this cell line, resulting in constitutive NRF2 activation [24]. NRF2 is a transcription factor that regulates the expression of a battery of antioxidant defense genes, including TR1. Thus, A549 cells represent a lung carcinoma with high expression of the Trx

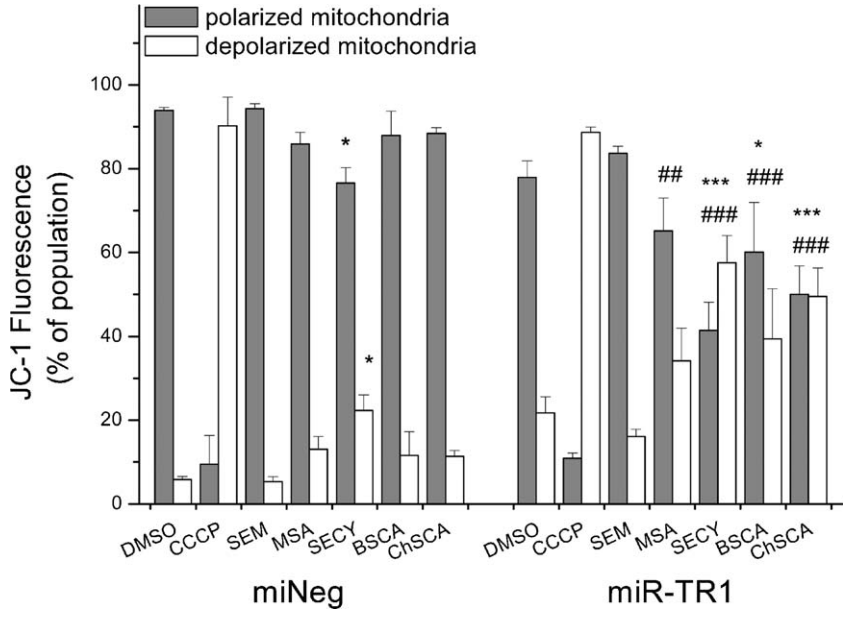

Fig. 8. TR1 knockdown increases selenocompound-mediated mitochondrial membrane depolarization. Determination of mitochondrial membrane potential by JC-1 after 48 h treatment. Compounds were used at the following concentrations: SEM, 20 μM; MSA, 1 μM; SECY, BSCA, and ChSCA, 5 μM. Data are expressed as % total population, with the 525 nm fluorescence population (JC-1 green) represented as depolarized mitochondria and the 575 nm fluorescence population (JC-1 red) represented as polarized mitochondria. Carbonyl cyanide 3-chlorophenylhydrazone (CCCP; 25 μM), a known mitochondrial membrane disrupter, served as positive control. (*) Indicates $p < 0.05$ versus matched DMSO vehicle control; (***) indicates $p < 0.001$ versus matched DMSO vehicle control; (##) indicates $p < 0.01$ versus matched miNeg treatment; (###) indicates $p < 0.001$ versus matched miNeg treatment.

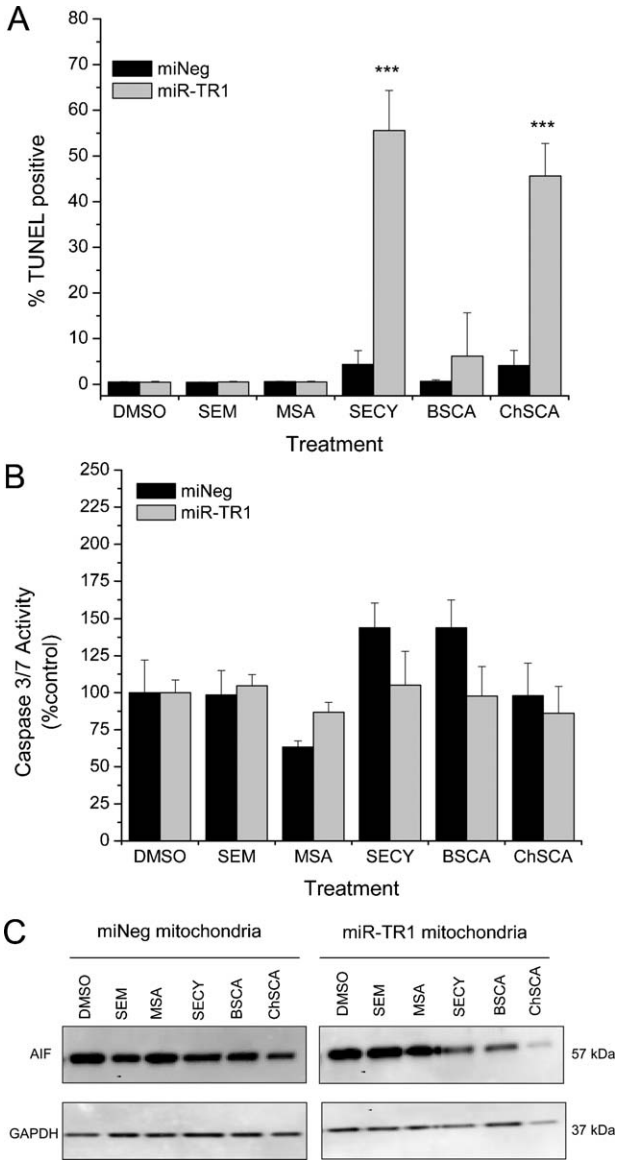

Fig. 9. SECY and the selenazolidines induce cell death through a caspase-independent mechanism. For all data shown, cells were treated at the following concentrations for 48 h: SEM, 20 μM; MSA, 1 μM; SECY, BSCA, and ChSCA, 5 μM. (A) Measure of DNA strand breaks by the TUNEL assay. 10,000 events were measured for each sample. Data shown are for BrdU positive, PI negative cell populations and are presented as % total population. (***) Indicates $p < 0.001$ versus matched DMSO vehicle control. All samples were analyzed at least in duplicate. (B) Caspase 3/7 activity. Data are presented as expressed as % matched DMSO vehicle control. No significance difference between treatment groups was found. (C) AIF protein expression in mitochondrial fractions. 1 μg mitochondrial protein was loaded for each sample. GAPDH was probed as a protein loading control. α-Tubulin protein was not detected (data not shown), indicating that the mitochondrial fractions were free of cytosolic contamination. The blot shown is representative of two individual experiments.

system and aberrant NRF2. Dysfunction of these antioxidant systems has been shown to be a factor in resistance to several anticancer drugs [8,10,35,36]. Altered expression levels of NRF2 and KEAP1 are common occurrences in NSCLC tumors and are associated with worse overall patient survival [24,37]. Of the lung tumors studied, 26% had nuclear NRF2 expression, 56% had undetectable or low KEAP1 expression, and 41% had a KEAP1 mutation. An additional study of NSCLC tumors found that almost half of the tumors studied had strong TR expression [4]. These NRF2, KEAP1, and TR1 expression patterns observed in patient tumor samples are similar to those of A549 cells, making this cell line an applicable model for many NSCLCs. In this study, we performed knockdown of a single NRF2-regulated antioxidant gene, TR1. There was no observable difference in A549 viability with TR1 knockdown alone in our study or a previous report [38]. We also observed a lack of effects on redox parameters and mitochondrial membrane integrity with TR1 knockdown alone. One explanation for this is the unregulated antioxidant response and increased reductive capacity of the A549 cell line. We extended the observation from the KEAP1 mutant phenotype under study with a comparison of the cytotoxic activity of SECY and ChSCA in H1666 cells. The selenazolidine, ChSCA, demonstrated cytotoxicity comparable to the miR-TR1 A549 cells.

Studies have demonstrated decreased anticancer drug resistance with NRF2 knockdown and the consequential global effects on NRF2-regulated gene transcription. We observed that knockdown of only one NRF2-regulated gene, TR1, was able to enhance selenocompound cytotoxicity. The data presented here demonstrate that selenocompounds exhibit differential cytotoxic effects in A549 cells with decreased TR1. TR1 knockdown only increased selenazolidine and SECY cytotoxicity as determined by cellular ATP content. Our clonogenic survival assays suggest that the long-term treatment with these compounds may preclude the advantage of TR1 attenuation; however, additional experiments, perhaps including xenograft studies, may be more applicable to determining if targeting TR1 while treating with redox active agents provides therapeutic advantage *in vivo*. TR1 attenuation did not alter the cytotoxicity of MSA, SEM, or *p*-XSC (data not shown for *p*-XSC). Increased sensitivity to MSA has been observed in the RKO colon cancer cell line with TR1 knockdown via an autophagic mechanism [12], indicating that while MSA can have increased cytotoxic properties with TR1 knockdown, these effects are tissue specific. We also investigated CDDP since the Trx system has been linked to its resistance. CDDP interacts with TR1 at the selenocystine residue, resulting in irreversible inhibition of the enzyme [39]. TR1 knockdown did not affect CDDP cytotoxicity in this study, indicating that other factors may be responsible for CDDP resistance *in vitro*, such as the glutaredoxin system that can be inhibited by the GSH adduct of CDDP. However, it was recently shown that CDDP with the organoselenium TR inhibitor ethaselen reduced tumor size in A549-grafted nude mice to a greater extent than CDDP alone [8], demonstrating that targeting TR1 in combination with redox active anticancer drugs is an effective strategy to reduce tumor growth *in vivo*.

Interestingly, the selenazolidines and SECY were the only compounds whose cytotoxicity was affected by TR1 expression. These compounds also increased ROS in a TR1 dependent manner, indicating a protective role for TR1 in A549 cells. TR1 has been shown to protect other cancer cell lines from oxidative species generated by hydrogen peroxide, radiation, and CCDP. It is also possible that knockdown of TR1 lowers the concentration at which selenocompounds function as pro-oxidants rather than antioxidants. The selenazolidines and SECY decreased intracellular GSH levels to the greatest extent (~90%). Given that these compounds decreased total GSH independent of TR1 status, it is not surprising that they also affected the Trx oxidation state regardless of TR1 expression. However, GSH depletion and Trx oxidation are unlikely to be solely responsible for the cell death mechanism, as these compounds altered these parameters to an equal extent in the miNeg cells but did not alter miNeg cell viability. Pretreatment with the antioxidants NAC and tiron did not decrease the sensitivity of A549 cells to the selenazolidines and SECY. Therefore, either the pretreatment regimen was ineffective or the ROS generation was a consequence rather than initiator of cell death. Cell death was also observed with depletion of both the TR1 and GSH systems in the absence of an external oxidative or

electrophilic insult, indicating the need for depletion of both these antioxidant systems to induce cell killing in the basally reduced A549 cell line. In one study, the depletion of TR1 and GSH together for 48 h did not result in A549 cell death [38]; we show here that it is necessary to maintain simultaneous depletion of these antioxidant systems out to 72 hrs to elicit cell death. This need for sustained antioxidant depletion further demonstrates the high reserve antioxidant capacity of the A549 cell line and presents a potential treatment strategy for these types of tumors.

As one SECY molecule contains two Se atoms, the Se content of one mole of SECY is twice that of compounds containing one Se atom, such as the selenazolidines. To ensure that the observed cytotoxic and redox effects of SECY were not merely a result of a higher Se concentration from this compound, ROS generation was evaluated for 2.5 μM SECY. This concentration provided an equivalent molar amount of Se as 5 μM BSCA or ChSCA. No increase in ROS was detected with 2.5 μM SECY in miR-TR1 cells (data not shown), indicating that the Se concentration itself is not solely responsible for the observed redox effects. Of course, this assessment of Se content and Se-mediated cytotoxicity cannot account for potential differences in absorption, metabolism and elimination that may exist among the selenocompounds *in vivo*. These parameters have yet to be assessed in an *in vivo* model system.

Mitochondrial dysfunction and AIF-induced cell death, such as that induced by the selenocompounds in this study, has been shown to be an effective method of killing chemoresistant NSCLC cell lines [40,41]. Consistent with our results, evidence for selenocompounds inducing a caspase-independent mechanism of cell death in transformed cells through mitochondrial pathways has been demonstrated, including AIF-mediated mechanisms for SECY and selenite [42–45]. In this work, we observed that selenocompounds in combination with TR1 knockdown can induce mitochondrial dysfunction at lower concentrations than those used in our previous study, even as the mitochondrial isoform remains intact. Since caspase-dependent mechanisms of cell death are not effective at killing resistant NSCLC cells, the caspase-independent mechanism indicated by our results presents an intriguing ability of the selenazolidines to induce cell death with decreased TR1 expression.

Selenazolidines are organoselenocompounds designed to release selenocysteine either enzymatically or through spontaneous hydrolysis [46]. Once selenocysteine is liberated, it can dimerize with itself to generate SECY. These prodrugs lack the chemical instability associated with selenocysteine, as selenocysteine can easily oxidize to diselenide. Selenaozlidines exhibit decreased cytoxicity and greater biological availability of Se in comparison to sodium selenite and SEM in cell culture [47,48] and comparable chemoprevention efficacy to SECY [49]. In this study, we utilized two selenazolidines, BSCA and ChSCA, which are thought to release selenocysteine through spontaneous hydrolysis and have demonstrated anticancer activity *in vivo*. Herein, we have demonstrated that the cytotoxic and redox modulatory properties of the selenazolidines relate to TR1 expression and mirror those of SECY.

In summary, our data demonstrate that TR1 knockdown increases the cytotoxicity of the selenocompounds BSCA, ChSCA, and SECY in A549 cells through a mitochondrial pathway. Further work to investigate the use of these compounds in combination with thioredoxin reductase inhibitors or current chemotherapies is of interest.

Acknowledgements

We wish to thank Drs. Frank Kotch and Jeanette Roberts at the University of Wisconsin-Madison for synthesizing BSCA and ChSCA, Dr. Andrea Bild for the H1666 cells, Dr. Hidenori Ichijo for the ASK1 constructs, and Matthew Honeggar for his work in generating the A549 miRNA cell lines. We also acknowledge the University of Utah Core Facilities by P30 CA042014 awarded to the Huntsman Cancer Institute. This work was supported by USPHS Grant CA115616 (PJM) and NIH NRSA Pre-doctoral Fellowship F31AT005041-02 (RLP).

References

[1] Yoo MH, Xu XM, Carlson BA, Patterson AD, Gladyshev VN, Hatfield DL. Targeting thioredoxin reductase 1 reduction in cancer cells inhibits self-sufficient growth and DNA replication. PLoS One 2007;2(10):e1112.
[2] Sun QA, Wu Y, Zappacosta F, Jeang KT, Lee BJ, Hatfield DL, et al. Redox regulation of cell signaling by selenocysteine in mammalian thioredoxin reductases. J Biol Chem 1999;274(35):24522–30.
[3] Schenk H, Klein M, Erdbrugger W, Droge W, Schulze-Osthoff K. Distinct effects of thioredoxin and antioxidants on the activation of transcription factors NF-kappa B and AP-1. Proc Natl Acad Sci U S A 1994;91(5):1672–6.
[4] Soini Y, Kahlos K, Napankangas U, Kaarteenaho-Wiik R, Saily M, Koistinen P, et al. Widespread expression of thioredoxin and thioredoxin reductase in non-small cell lung carcinoma. Clin Cancer Res 2001;7(6):1750–7.
[5] Kakolyris S, Giatromanolaki A, Koukourakis M, Powis G, Souglakos J, Sivridis E, et al. Thioredoxin expression is associated with lymph node status and prognosis in early operable non-small cell lung cancer. Clin Cancer Res 2001;7(10):3087–91.
[6] Fernandes AP, Capitanio A, Selenius M, Brodin O, Rundlof AK, Bjornstedt M. Expression profiles of thioredoxin family proteins in human lung cancer tissue: correlation with proliferation and differentiation. Histopathology 2009;55(3):313–20.
[7] Yoo MH, Xu XM, Carlson BA, Gladyshev VN, Hatfield DL. Thioredoxin reductase 1 deficiency reverses tumor phenotype and tumorigenicity of lung carcinoma cells. J Biol Chem 2006;281(19):13005–8.
[8] Tan Q, Li J, Yin HW, Wang LH, Tang WC, Zhao F, et al. Augmented antitumor effects of combination therapy of cisplatin with ethaselen as a novel thioredoxin reductase inhibitor on human A549 cell in vivo. Invest New Drugs 2010;28(3):205–15.
[9] Smart DK, Ortiz KL, Mattson D, Bradbury CM, Bisht KS, Sieck LK, et al. Thioredoxin reductase as a potential molecular target for anticancer agents that induce oxidative stress. Cancer Res 2004;64(18):6716–24.
[10] Sasada T, Nakamura H, Ueda S, Sato N, Kitaoka Y, Gon Y, et al. Possible involvement of thioredoxin reductase as well as thioredoxin in cellular sensitivity to cis-diamminedichloroplatinum (II). Free Radic Biol Med 1999;27(5–6):504–14.
[11] Madeja Z, Sroka J, Nystrom C, Bjorkhem-Bergman L, Nordman T, Damdimopoulos A, et al. The role of thioredoxin reductase activity in selenium-induced cytotoxicity. Biochem Pharmacol 2005;69(12):1765–72.
[12] Honeggar M, Beck R, Moos PJ. Thioredoxin reductase 1 ablation sensitizes colon cancer cells to methylseleninate-mediated cytotoxicity. Toxicol Appl Pharmacol 2009;241(3):348–55.
[13] Ceccarelli J, Delfino L, Zappia E, Castellani P, Borghi M, Ferrini S, et al. The redox state of the lung cancer microenvironment depends on the levels of thioredoxin expressed by tumor cells and affects tumor progression and response to prooxidants. Int J Cancer 2008;123(8):1770–8.
[14] Reid ME, Duffield-Lillico AJ, Slate E, Natarajan N, Turnbull B, Jacobs E, et al. The nutritional prevention of cancer: 400 mcg per day selenium treatment. Nutr Cancer 2008;60(2):155–63.
[15] Lippman SM, Klein EA, Goodman PJ, Lucia MS, Thompson IM, Ford LG, et al. Effect of selenium and vitamin E on risk of prostate cancer and other cancers: the Selenium and Vitamin E Cancer Prevention Trial (SELECT). JAMA 2009;301(1):39–51.
[16] Duffield-Lillico AJ, Dalkin BL, Reid ME, Turnbull BW, Slate EH, Jacobs ET, et al. Selenium supplementation, baseline plasma selenium status and incidence of prostate cancer: an analysis of the complete treatment period of the Nutritional Prevention of Cancer Trial. BJU Int 2003;91(7):608–12.
[17] Clark LC, Combs Jr GF, Turnbull BW, Slate EH, Chalker DK, Chow J, et al. Effects of selenium supplementation for cancer prevention in patients with carcinoma of the skin. A randomized controlled trial. Nutritional Prevention of Cancer Study Group. JAMA 1996;276(24):1957–63.
[18] Swede H, Dong Y, Reid M, Marshall J, Ip C. Cell cycle arrest biomarkers in human lung cancer cells after treatment with selenium in culture. Cancer Epidemiol Biomarkers Prev 2003;12(11 Pt 1):1248–52.
[19] Li GX, Lee HJ, Wang Z, Hu H, Liao JD, Watts J, et al. Superior in vivo inhibitory efficacy of methylseleninic acid against human prostate cancer over selenomethionine or selenite. Carcinogenesis 2008;29(5):1005–12.
[20] Prokopczyk B, Amin S, Desai DH, Kurtzke C, Upadhyaya P, El-Bayoumy K. Effects of 1,4-phenylenebis(methylene)selenocyanate and selenomethionine on 4-(methylnitrosamino)-1-(3-pyridyl)-1-butanone-induced tumorigenesis in A/J mouse lung. Carcinogenesis 1997;18(9):1855–7.
[21] El-Bayoumy K, Rose DP, Papanikolaou N, Leszczynska J, Swamy MV, Rao CV. Cyclooxygenase-2 expression influences the growth of human large and small cell lung carcinoma lines in athymic mice: impact of an organoselenium compound on growth regulation. Int J Oncol 2002;20(3):557–61.
[22] El-Bayoumy K, Das A, Narayanan B, Narayanan N, Fiala ES, Desai D, et al. Molecular targets of the chemopreventive agent 1,4-phenylenebis (methy-

lene)-selenocyanate in human non-small cell lung cancer. Carcinogenesis 2006;27(7):1369–76.
[23] Franklin MR, Moos PJ, El-Sayed WM, Aboul-Fadl T, Roberts JC. Pre- and post-initiation chemoprevention activity of 2-alkyl/aryl selenazolidine-4(R)-carboxylic acids against tobacco-derived nitrosamine (NNK)-induced lung tumors in the A/J mouse. Chem Biol Interact 2007;168(3):211–20.
[24] Singh A, Misra V, Thimmulappa RK, Lee H, Ames S, Hoque MO, et al. Dysfunctional KEAP1-NRF2 interaction in non-small-cell lung cancer. PLoS Med 2006;3(10):e420.
[25] El-Sayed W, Aboul-Fadl T, Lamb JG, Roberts JC, Franklin MR. Acute effects of novel selenazolidines on murine chemoprotective enzymes. Chem Biol Interact 2006;162(1):31–42.
[26] Moos PJ, Edes K, Cassidy P, Massuda E, Fitzpatrick FA. Electrophilic prostaglandins and lipid aldehydes repress redox-sensitive transcription factors p53 and hypoxia-inducible factor by impairing the selenoprotein thioredoxin reductase. J Biol Chem 2003;278(2):745–50.
[27] Poerschke RL, Franklin MR, Moos PJ. Modulation of redox status in human lung cell lines by organoselenocompounds: selenazolidines, selenomethionine, and methylseleninic acid. Toxicol In Vitro 2008;22(7):1761–7.
[28] Edes K, Cassidy P, Shami PJ, Moos PJ. JS-K, a nitric oxide prodrug, has enhanced cytotoxicity in colon cancer cells with knockdown of thioredoxin reductase 1. PLoS One 2010;5(1):e8786.
[29] Bersani NA, Merwin JR, Lopez NI, Pearson GD, Merrill GF. Protein electrophoretic mobility shift assay to monitor redox state of thioredoxin in cells. Methods Enzymol 2002;347:317–26.
[30] Watson WH, Heilman JM, Hughes LL, Spielberger JC. Thioredoxin reductase-1 knock down does not result in thioredoxin-1 oxidation. Biochem Biophys Res Commun 2008;368(3):832–6.
[31] Saitoh M, Nishitoh H, Fujii M, Takeda K, Tobiume K, Sawada Y, et al. Mammalian thioredoxin is a direct inhibitor of apoptosis signal-regulating kinase (ASK) 1. Embo J 1998;17(9):2596–606.
[32] Ichijo H, Nishida E, Irie K, ten Dijke P, Saitoh M, Moriguchi T, et al. Induction of apoptosis by ASK1, a mammalian MAPKKK that activates SAPK/JNK and p38 signaling pathways. Science 1997;275(5296):90–4.
[33] Susin SA, Lorenzo HK, Zamzami N, Marzo I, Snow BE, Brothers GM, et al. Molecular characterization of mitochondrial apoptosis-inducing factor. Nature 1999;397(6718):441–6.
[34] Petrelli NJ, Winer EP, Brahmer J, Dubey S, Smith S, Thomas C, et al. Clinical Cancer Advances 2009: major research advances in cancer treatment, prevention, and screening–a report from the American Society of Clinical Oncology. J Clin Oncol 2009;27(35):6052–69.
[35] Singh A, Boldin-Adamsky S, Thimmulappa RK, Rath SK, Ashush H, Coulter J, et al. RNAi-mediated silencing of nuclear factor erythroid-2-related factor 2 gene expression in non-small cell lung cancer inhibits tumor growth and increases efficacy of chemotherapy. Cancer Res 2008;68(19):7975–84.
[36] Homma S, Ishii Y, Morishima Y, Yamadori T, Matsuno Y, Haraguchi N, et al. Nrf2 enhances cell proliferation and resistance to anticancer drugs in human lung cancer. Clin Cancer Res 2009;15(10):3423–32.
[37] Solis LM, Behrens C, Dong W, Suraokar M, Ozburn NC, Moran CA, et al. Nrf2 and Keap1 abnormalities in non-small cell lung carcinoma and association with clinicopathologic features. Clin Cancer Res 2010;16(14):3743–53.
[38] Eriksson SE, Prast-Nielsen S, Flaberg E, Szekely L, Arner ES. High levels of thioredoxin reductase 1 modulate drug-specific cytotoxic efficacy. Free Radic Biol Med 2009;47(11):1661–71.
[39] Arner ES, Nakamura H, Sasada T, Yodoi J, Holmgren A, Spyrou G. Analysis of the inhibition of mammalian thioredoxin, thioredoxin reductase, and glutaredoxin by cis-diamminedichloroplatinum (II) and its major metabolite, the glutathione-platinum complex. Free Radic Biol Med 2001;31(10):1170–8.
[40] Joseph B, Marchetti P, Formstecher P, Kroemer G, Lewensohn R, Zhivotovsky B. Mitochondrial dysfunction is an essential step for killing of non-small cell lung carcinomas resistant to conventional treatment. Oncogene 2002;21(1):65–77.
[41] Gallego MA, Joseph B, Hemstrom TH, Tamiji S, Mortier L, Kroemer G, et al. Apoptosis-inducing factor determines the chemoresistance of non-small-cell lung carcinomas. Oncogene 2004;23(37):6282–91.
[42] Rudolf E, Rudolf K, Cervinka M. Selenium activates p53 and p38 pathways and induces caspase-independent cell death in cervical cancer cells. Cell Biol Toxicol 2008;24(2):123–41.
[43] Kim TS, Yun BY, Kim IY. Induction of the mitochondrial permeability transition by selenium compounds mediated by oxidation of the protein thiol groups and generation of the superoxide. Biochem Pharmacol 2003;66(12):2301–11.
[44] Jonsson-Videsater K, Bjorkhem-Bergman L, Hossain A, Soderberg A, Eriksson LC, Paul C, et al. Selenite-induced apoptosis in doxorubicin-resistant cells and effects on the thioredoxin system. Biochem Pharmacol 2004;67(3):513–22.
[45] Chen T, Wong YS. Selenocystine induces caspase-independent apoptosis in MCF-7 human breast carcinoma cells with involvement of p53 phosphorylation and reactive oxygen species generation. Int J Biochem Cell Biol 2009;41(3):666–76.
[46] Xie Y, Short MD, Cassidy PB, Roberts JC. Selenazolidines as novel organoselenium delivery agents. Bioorg Med Chem Lett 2001;11(22):2911–5.
[47] Short MD, Xie Y, Li L, Cassidy PB, Roberts JC. Characteristics of selenazolidine prodrugs of selenocysteine: toxicity and glutathione peroxidase induction in V79 cells. J Med Chem 2003;46(15):3308–13.
[48] Li L, Xie Y, El-Sayed WM, Szakacs JG, Roberts JC. Characteristics of selenazolidine prodrugs of selenocysteine: toxicity, selenium levels, and glutathione peroxidase induction in A/J mice. Life Sci 2004;75(4):447–59.
[49] Li L, Xie Y, El-Sayed WM, Szakacs JG, Franklin MR, Roberts JC. Chemopreventive activity of selenocysteine prodrugs against tobacco-derived nitrosamine (NNK) induced lung tumors in the A/J mouse. J Biochem Mol Toxicol 2005;19(6):396–405.